

# COMPRESSIBLE MULTIMATERIAL FLOWS

F. Bernard<sup>1</sup>, A. de Brauer<sup>2</sup>, A. Iollo<sup>1,a)</sup>, T. Milcent<sup>3</sup> and H. Telib<sup>4</sup>

<sup>1</sup>IMB, University of Bordeaux, UMR CNRS 5251; INRIA Memphis Team, F-33400 Talence, France

<sup>2</sup>IIHR, University of Iowa, Iowa City, Iowa 52242-1585, USA

<sup>3</sup>I2M, University of Bordeaux, UMR CNRS 5295; Arts et Métiers Paristech, F-33600 Pessac, France

<sup>4</sup>Optimad Engineering, I-10143, Turin, Italy.

a)Corresponding and presenting author: angelo.iollo@inria.fr

## 1 ABSTRACT

We consider hyperbolic models of gas flows past unsteady or elastic-plastic solids. The numerical framework is based on hierarchical cartesian grids, implicit representation of fluid-solid interfaces, stable and accurate discretization schemes. We present examples relative to compressible flows in unsteady aerodynamics, high-speed elastoplastic impacts and rarefied re-entry flows.

## 2 MODELS

### 2.1 *Elasto-plastic materials*

We consider two models. The first is relative to a compressible elastic-plastic continuum medium. This model was introduced in the literature thanks to several authors [6, 10, 9, 3, 5]. We follow here the formulation presented in [7, 4] and extend it to plasticity modelling. The equations of mass, momentum, deformation and energy conservation are given by

$$\begin{cases} \partial_t \rho + \operatorname{div}_x(\rho u) = 0 \\ \partial_t(\rho u) + \operatorname{div}_x(\rho u \otimes u - \sigma) = 0 \\ \partial_t(\nabla_x Y) + \nabla_x(u \cdot \nabla_x Y) = 0 \\ \partial_t(\rho e) + \operatorname{div}_x(\rho e u - \sigma^T u) = 0 \end{cases} \quad (1)$$

Here  $Y(x, t)$  are the backward characteristics that for a time  $t$  and a point  $x$  in the deformed configuration, give the corresponding initial point.

We assume that the internal energy per unit mass  $\varepsilon = e - \frac{1}{2}|u|^2$  is the sum of a term accounting for volume deformation that depends on  $\rho$  and entropy  $s$ , and a term accounting for isochoric deformation depending on the modified left Cauchy-Green tensor  $\bar{B}$  given by  $\bar{B}(x, t) = [\nabla_x Y]^{-1}[\nabla_x Y]^{-T} / J^{\frac{2}{3}}(x, t)$ ,  $J(x, t) = \det([\nabla_x Y])^{-1}$ . A general constitutive law that models gas, fluids and elastic solids is then given by

$$\varepsilon(\rho, s, \nabla_x Y) = \frac{\kappa(s)\rho^{\gamma-1}}{\gamma-1} + \frac{p_\infty}{\rho} + \frac{\chi}{\rho_0}(\operatorname{Tr}(\bar{B}) - 3) \quad (2)$$

where the first term accounts for a perfect gas, the second for a stiffened gas (e.g. water) and the third for a neo-hookean elastic solid. The Cauchy stress tensor is obtained from the above constitutive law. Here  $\kappa(s) = \exp(s/c_v)$  and  $c_v, \gamma, p_\infty, \chi$  are positive constants that characterize a given material. Compressible Euler equations are included in this model.

Plasticity describes the deformation of a material undergoing non-reversible changes of shape in response to applied forces. The deformation can be modeled by the composition of a plastic and an elastic deformation [8]. We introduce the backward characteristics for elastic and plastic deformations denoted by  $Y^e$  and  $Y^p$ , respectively. Let us define the deviatoric part of the stress tensor  $\operatorname{dev}(\sigma) = \sigma - \frac{\operatorname{Tr}(\sigma)}{3}I$ . Experimentally plasticity occurs when the stress exceeds a critical value. The yield function of von Misses  $f_{VM}(\sigma) = |\operatorname{dev}(\sigma)|^2 - \frac{2}{3}(\sigma_y)^2$  defines a yield surface  $f_{VM}(\sigma) = 0$  where  $\sigma_y$  is the plastic yield limit. We restrict ourselves to the case of perfect plasticity where  $\sigma_y$  is a constant.

A constitutive law for plasticity [9, 1] is defined by

$$\partial_t(\nabla_x Y^e) + \nabla_x(u \cdot \nabla_x Y^e) = \frac{1}{\chi\tau}[\nabla_x Y^e]\text{dev}(\sigma) \quad (3)$$

where  $\chi$  is the shear modulus and  $\tau$  is the relaxation time of the plastic process. Beyond yield, plasticity appears as a source term in the equation of deformations and can be seen as a penalization of the deviatoric part of  $\sigma$ .

## 2.2 Rarefied polyatomic flows

We consider a BGK model for polyatomic gases. Going from monoatomic to polyatomic gases implies that additional energy degrees of freedom are considered. In the classical BGK model, only translational energy degrees of freedom are taken into account. We now consider a more general case with  $d$  energy degrees of freedom including rotational and vibrational energy degrees of freedom. The idea is to consider these additional energy degrees of freedom in the expression of the maxwellian distribution function. Moreover, we consider a general case where the energy is not equally distributed between the energy degrees of freedom. Let  $\boldsymbol{\eta} \in \mathbb{R}^d$  the vector of the energy degrees of freedom ( $\boldsymbol{\eta} = \boldsymbol{\xi}$  for the BGK model),  $\bar{\boldsymbol{\eta}} \in \mathbb{R}^d$  the macroscopic value on which the equilibrium function is centered ( $\mathbf{U}$  in the case of the BGK model),  $\boldsymbol{\lambda} \in \mathbb{R}^d$  the vector of the coefficient giving the distribution of the energy between the degrees of freedom ( $1/2T$  in the case of the BGK model for the three translational energy degrees of freedom). The model reads:

$$\frac{\partial f}{\partial t} + \boldsymbol{\xi} \cdot \nabla_x f = \frac{1}{\tau}(M_f - f) \quad (4)$$

$$M_f(\mathbf{x}, \boldsymbol{\eta}, t) = \rho(\mathbf{x}, t) \prod_{k=1,d} \left(\frac{\lambda_k}{\pi}\right)^{1/2} \exp\left(-(\lambda_k(\eta_k - \bar{\eta}_k))^2\right) \quad (5)$$

The evolution of  $\boldsymbol{\lambda}$  is governed by the equation of energy conservation and by a relaxation of the equilibrium temperature of the rotational degrees of freedom,  $\Theta$ , towards the equilibrium temperature of the translational degrees of freedom denoted  $\Lambda$ :

$$\partial_t \Theta + \mathbf{U} \cdot \nabla \Theta = \frac{1}{Z_r \tau}(\Lambda - \Theta) \quad (6)$$

where  $Z_r$  is a given parameter corresponding the rotation frequency of the gas molecules.

## 3 NUMERICAL ILLUSTRATIONS

### 3.1 Plastic impact

We have extended the scheme described in [7, 4] to model elasto-plastic flows. The scheme is based on a sharp-interface locally non-conservative approximate Riemann solver that has been validated in 2D and 3D.

Here we show a 2D test case where an iron circular projectile is impacting onto an aluminium flat plate fixed to the upper and lower boundaries of the computational domain. The initial horizontal velocity of the iron projectile is  $1000m \cdot s^{-1}$ . The physical parameters for the different materials are found in the literature and the computational domain is  $[-0.3, 0.7]m \times [-0.4, 0.4]m$ . The computation is performed on a  $2000 \times 1600$  mesh with 144 processors. Homogeneous Neumann conditions are imposed on the left and right borders and embedded on the top and bottom.

The results are presented in Fig. 2 depicting a Schlieren image and the value of the von Mises criteria  $|\text{dev}(\sigma)|^2 - \frac{2}{3}(\sigma_y)^2$  at a time steps corresponding to an early impact stage and to an highly deformed plastic state. A longitudinal wave propagating in the plate is followed by a shear wave that causes the plasticity of the material. We can observe that the plate, initially straight, is strongly deformed and forms a long filament; the projectile, initially round, is considerably flattened. Shock waves and contact discontinuities characterise the air flow.

### 3.2 Capsule re-entry

A capsule based on Apollo design is immersed in a rarefied gas flow at Mach 5. Free flow conditions are imposed on the boundaries of the domain except at the inlet where the state is imposed. On the capsule we enforce a zero velocity (with respect to the capsule) and a temperature equal to 1 in dimensionless variables. The capsule will then move according to the torque due to the fluid force on the body until an equilibrium depending on the position of the center of mass is

attained. The numerical scheme for a monoatomic gas is described in [2]. We extend that scheme to polyatomic gases. The computation is performed on a  $80 \times 80 \times 80$  grid in space and a  $21 \times 21 \times 21$  grid in velocity with a Knudsen number of  $10^{-2}$  with 128 processors. The simulation took about 2 days.

## 4 CONCLUSIONS

In the proposed presentation we will describe the hierarchical schemes used for these simulations. In particular, we will detail how to recover consistency and accuracy at the unsteady interfaces that arbitrarily cross the grid. Additional results in 3D aerodynamics will be presented.

## References

- [1] P.T. Barton, R. Deiterding, D. Meiron, and D. Pullin. Eulerian adaptive finite-difference method for high-velocity impact and penetration problems. Journal of Computational Physics, 240(C):76–99, 2013. (Cited on page 2.)
- [2] F. Bernard, A. Iollo, and G. Puppo. Accurate Asymptotic Preserving Boundary Conditions for Kinetic Equations on Cartesian Grids. Journal of Scientific Computing, January 2015. (Cited on page 3.)
- [3] G.H. Cottet, E. Maitre, and T. Milcent. Eulerian formulation and level set models for incompressible fluid-structure interaction. ESAIM: Mathematical Modelling and Numerical Analysis, 42:471–492, 2008. (Cited on page 1.)
- [4] A. de Brauer, A. Iollo, and T. Milcent. A cartesian scheme for compressible multimaterial models in 3d. Journal of Computational Physics, 313(C):121–143, May 2016. (Cited on pages 1 and 2.)
- [5] N. Favrie, S.L. Gavrilyuk, and R. Saurel. Solid-fluid diffuse interface model in cases of extreme deformations. Journal of Computational Physics, 228(16):6037–6077, 2009. (Cited on page 1.)
- [6] S.K. Godunov. Elements of continuum mechanics. Nauka Moscow, 1978. (Cited on page 1.)
- [7] Y. Gorsse, A. Iollo, T. Milcent, and H. Telib. A simple cartesian scheme for compressible multimaterials. Journal of Computational Physics, 272:772–798, 2014. (Cited on pages 1 and 2.)
- [8] E.H. Lee and D.T. Liu. Finite-strain elastic-plastic theory with application to plane-wave analysis. Journal of Applied Physics, 38(1):19–27, 1967. (Cited on page 1.)
- [9] G.H. Miller and P. Colella. A high-order eulerian godunov method for elastic-plastic flow in solids. Journal of Computational Physics, 167(1):131–176, 2001. (Cited on pages 1 and 2.)
- [10] B.J. Plohr and D.H. Sharp. A conservative eulerian formulation of the equations for elastic flow. Advances in Applied Mathematics, 9:481–499, 1988. (Cited on page 1.)

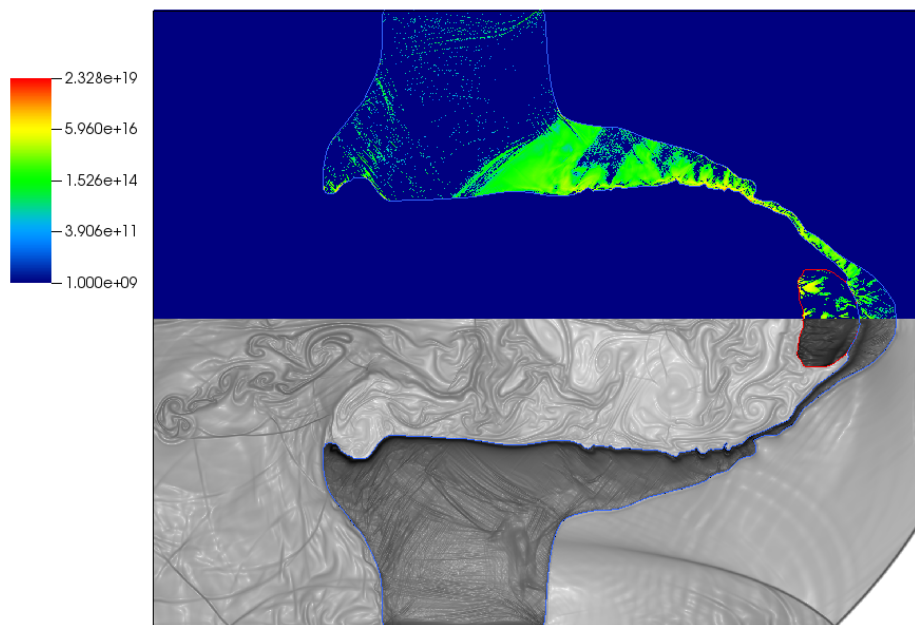
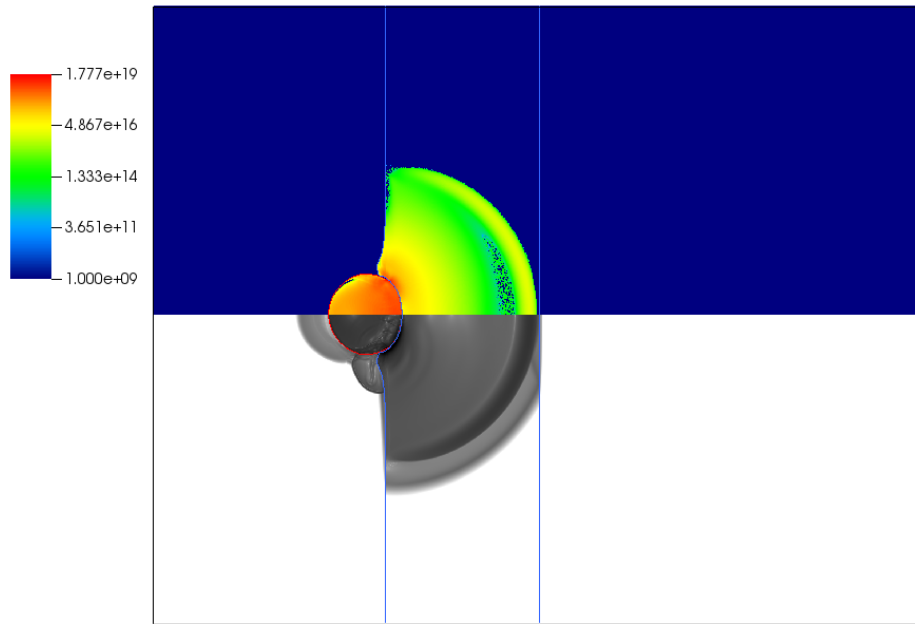


**Figure 1. Iron round projectile on an aluminium shield in air. Schlieren image and von Mises criterium at  $t = .03\text{ms}$  and  $t = 1.04\text{ms}$**

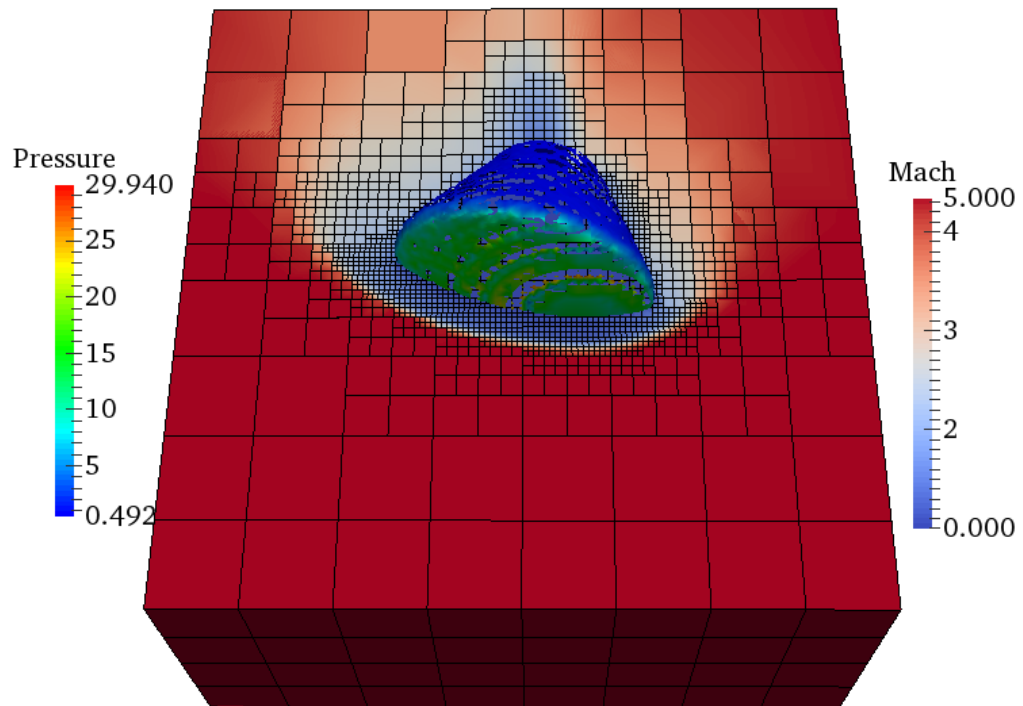


**Figure 2. Octree simulation of a re-entry capsule in a rarefied polyatomic gas.**